Descattering of Transmissive Observation using Parallel High-frequency Illumination

Kenichiro Tanaka[1] Yasuhiro Mukaigawa[1] Yasuyuki Matsushita[2] Yasushi Yagi[1]
[1]Institute of Scientific and Industrial Research, Osaka University, Japan
[2]Microsoft Research Asia
http://www.am.sanken.osaka-u.ac.jp/

Abstract

The inner structures of an object can be measured by capturing transmissive images. However, the recorded images of a translucent object tend to be unclear due to strong scattering of light inside the object. In this paper, we propose a descattering approach based on Parallel High-frequency Illumination. We show in this paper that the original high-frequency illumination method and the various extended techniques can be uniformly defined as a separation of overlapped and non-overlapped light rays. Also, we show that transmissive light rays do not overlap each other by constructing a parallel projection/measurement system for performing both illumination and observation. We have developed a measurement system that consists of a camera and projector with telecentric lenses and have evaluated descattering effects by extracting transmissive light rays.

1. Introduction

When recording transmissive observations of a translucent object, captured images tend to be unclear due to strong scattering. The scattering is caused by collisions of light rays with tiny particles in the medium that diffuses light rays, and is inevitable in diverse translucent objects. Therefore, for recording a clear transmissive images, effective descattering techniques are needed.

Figure 1 shows examples of transmissive images. A nail in a piece of food is shown in (a). There is high demand to check for foreign objects inside products in the food industry where transimissive imaging can help. Another example in (b) shows vein patterns inside a hand. Transimissive imaging is also useful for the purposes of visualization of the living body, measurement of blood oxigen levels [1], and security purposes. In such application domains, capability of recording clear transmissive images plays an important role.

There are various approaches for descattering in the field of computational photography via software post-processing and/or specially designed imaging setups. Gilvert and Pernicka [4] and Treibitz and Schechner [12] have shown that circular polarizers can be used for reducing back-scattering from the scene. The techniques are shown to be useful; however, the methods are limited to scenes where scattered light rays are well polarized. Narasimhan *et al*. [9] have sharpened images of a scene in muddy liquid by precisely modeling of single scattering, which works well for the scenes that do not contain multiple scattering. Fuchs *et al*. [3] used a projector for descattering. Kim *et al*. [5] propose a method for sharpning transmissive images using anglular information obtained by using a light field camera. Wu *et al*. [14] used a femto-laser and a streak camera for image decomposition to achieve a similar goal.

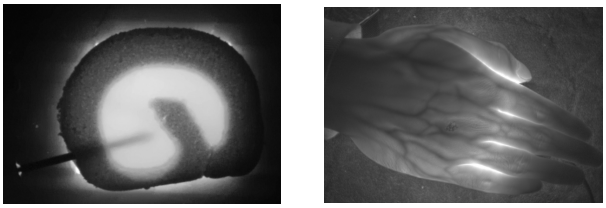

(a) Foreign object in food (b) Vein pattern

Figure 1. Examples of transmissive image.

In this paper, we propose a *Parallel High-frequency Illumination* method which sharpens transmissive images by separating the transmissive and scattered lights. We show in this paper that transmissive and scattered lights can be separated based on angular and positional clues. We then show that the original high-frequency illumination method proposed by Nayar *et al*. [10] and several extended methods [6, 8, 15] can be uniformly defined as a separation of the overlapped and non-overlapped rays. We finally evaluate the effectiveness of the pararell projection approach to separating transmissive and scattered lights via experiments.

2. Related Work

Using high transmittance wavelengths

X-ray imaging is usually used to obtain clear transmissive images, because it has a high transmittance aspect and rarely has scattering characteristics. However, the applicability of this method is limited because X-rays have an associated risk of radiation exposure.

Near infra-red light is also used for living body imaging because of its high transmittance. Vein authentication for security purpose is one example of this type of imaging. In the medical field, the difference in the absorption properties of near infra-red light between oxy-hemoglobin and deoxy-hemoglobin are used to measure blood oxygen levels [1]. Our goal is to obtain sharp images by removing scattering lights by using visible or infra-red light and special optics.

Using parallel light rays

In the optical measurement field, parallel light is traditionally used. Shadowgraphy [11] is a volumetric density distribution imaging method based on the detection of slight directional change of light rays caused by differences of refractive index in the medium. Although schlieren method [11] is similar to shadowgraphy, it cuts some parallel rays at their focal point with a knife edge and can visualize the density distributions with higher contrast. Hence, the schlieren method has been used for scattering measurements [2]. Recently, schlieren photography with light field probes [13] has been proposed to produce ray-ray correspondences.

In this research, we also use the indication that a parallel ray changes its direction because of scattering, and the optical setting is also similar. However, while shadowgraphy and schlieren method use only the directional clue, we use both the directional and positional clues by combining them with high-frequency illumination. Therefore, we can separate the transmissive and scattered lights more efficiently.

3. Parallel High-frequency Illumination

3.1. Transmissive Images

Transmissive image such as those in Fig. 1 can be obtained by placing a camera and a light source on opposite sides of the translucent object. The lights observed by the camera contain two components. One is the *transmissive light*, which passes straight through the scattering object. The other is the *scattered light*, which has various path changes caused by collisions with tiny particles. While the former component shows the internal structures in a translucent object directly, the latter component disturbs the clarity of the observation. To obtain a clear transmissive image, we need to eliminate the scattering lights and extract only the transmissive lights.

Before separating the transmissive and scattered lights, we must clarify the differences between the two components and determine the clues that can be used for our purposes. We summarize several clues for separation of the two components and introduce some conventional methods in the following.

Polarization clue

When the incident light is polarized, the transmissive and scattered lights have different polarization characteristics, as shown in Fig. 2 (a). While transmissive lights maintain their polarization because they are not affected by the object, the polarization can be gradually lost because of the collisions with tiny particles. Therefore, scattered lights which have bounced several times become only partially polarized, and the polarization is perfectly lost after multiple repeated bounces. Based on this difference, the scattered light can be reduced by the use of two co-linear polarizers [12].

Angle clue

Lights are emitted from an observed point to various directions, as shown in Fig. 2 (b). This emission angle is different for the transmissive and scattered lights. Because the path of the transmissive light does not change when passing through the object, the emitted light has the same direction as the incident light. However, the scattered light path has various changes caused by collisions, and thus the emission direction also changes. Based on this difference, Kim *et al*. [5] estimated the intensity of the transmissive light from angular observation using a light field camera. Brogili *et al*. [2] applied the schlieren method, which obscures the transmitted ray by using a knife edge, to measure the scattering lights.

Position clue

Scattered and transmissive lights have difference about emission positions, as shown in Fig. 2 (c). While the transmissive light is emitted on the same line as the incident light, the scattered light is emitted from various positions because it has been spread by the scattering objects. If the incident light is a narrow beam, then the transmissive light is observed as a pointed peak. When the incident point of the beam shifts slightly, the position of the observed transmissive light also shifts. However, the scattered light spreads smoothly, and a slight shift in the incident beam does not affect to the observation.

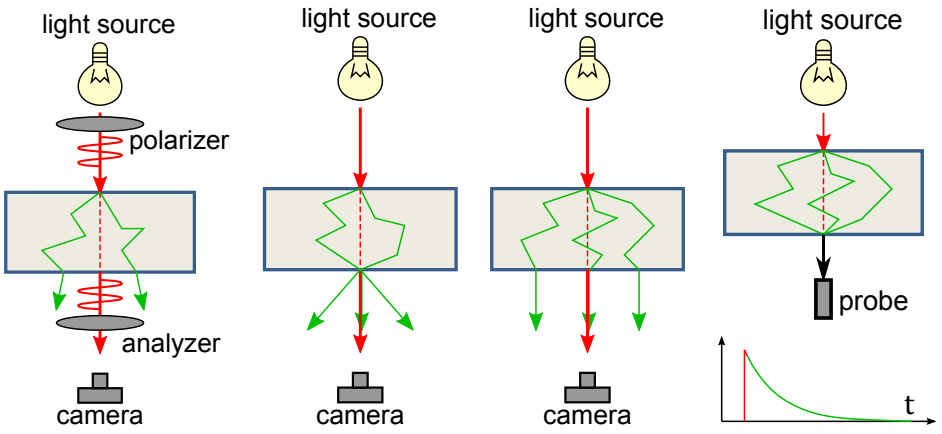

(a) Polarization (b) Angle (c) Position (d) Time

Figure 2. Differences between transmissive and scattered lights.

Other clues

Other clues have been also used for the separation. For example, the path length of scattered light rays obviously becomes longer than that of transmissive light rays, as shown in Fig. 2 (d). Therefore, the transmissive lights arrive earlier than the scattered lights. By using an ultra high speed sensor such as a streak tube, the two components can be separated based on this time clue [14]. A wavelength clue can also be used. Because the scattering and absorption depend on the wavelength, multi-band illumination is used for deblurring [7].

3.2. Parallel projection system

Our aim is to sharpen the transmissive images effectively based on the differences between the transmissive and scattered lights. As explained above, there are several clues that can help to detect the separation of these lights. However, there is no single perfect way. For example, the angle clue cannot be used to distinguish transmissive lights from straight-line scattered lights. Similarly, the position clue cannot be used to distinguish transmissive lights from scattered lights that are emitted from the same position.

To overcome this problem, we use a combination of both the angle and the position clues. To combine the different types of clues, we have designed a special optical system that can illuminate and observe high-frequency patterns *in parallel*, as shown in Fig. 3 (a). This system can also easily combine the polarization and wavelength clues by using a polarizer and a near infra-red light source, and thus we can use many differences as possible.

Two optical designs are used to realize the parallel high-frequency illumination. The first uses telecentric lenses, as shown in Fig. 3 (a). Although telecentric lenses are expensive and the viewing area becomes narrow, a variety of

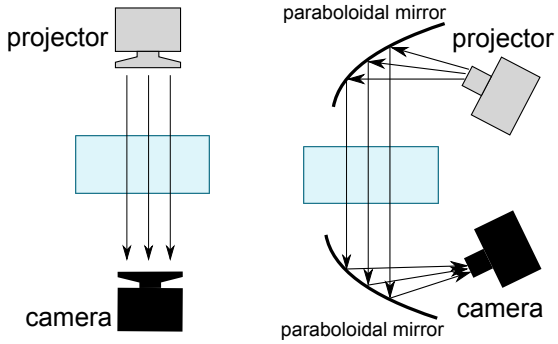

(a) Telecentric lenses (b) Paraboloidal mirrors

Figure 3. Optical design for parallel projection.

lenses are commercially available and this design is easy to configure. The other design uses paraboloidal mirrors, as shown in Fig. 3 (b). Although paraboloidal mirrors are low cost and the viewing area can easily be extended, it is necessary to precisely align the paraboloid's focal point to the optical centers of both the camera and the projector. In practice, we can select the design according to the size of the scene, the cost, and the difficulty of the setup.

3.3. Decomposition of transmissive and scattered lights

Let us assume that $L[c]$ is the light intensity observed by a camera at pixel c. L can be expressed as

$$L[c] = L_t[c] + L_s[c] \tag{1}$$

where $L_t[c]$ and $L_s[c]$ are the intensities of the transmissive and scattered lights at pixel c of the camera respectively.

Our method separates the transmissive and scattered lights by projecting effectively small checkered pattern, a similar way to the original method [10], but in parallel. When the phase of the projected pattern changes slightly, L_t also changes, but L_s rarely changes. Therefore, we can separate the light components based on this difference. We assume that the numbers of white and black pixels of the projected pattern are same. When the projected pattern is shifted, the maximum intensity $L_{max}[c]$ and the minimum intensity $L_{min}[c]$ of all observations are expressed as

$$L_{max}[c] = L_t[c] + \frac{1}{2}L_s[c], \tag{2}$$

$$L_{min}[c] = \frac{1}{2}L_s[c]. \tag{3}$$

From these relations, the transmissive and scattered lights can be computed as

$$L_t[c] = L_{max}[c] - L_{min}[c], \tag{4}$$

$$L_s[c] = 2L_{min}[c]. \tag{5}$$

We call this separation method the *Parallel High-frequency Illumination* method.

4. Separated components

4.1. Overlapped and non-overlapped rays

Nayar *et al*. [10] proposed the original high-frequency illumination method that separates the direct and global components. However, the photometric factors that directly correspond to the direct and global components depend on the settings of illumination and observation. Every separation method has a different scheme for pattern projection. The separable components are also different. However, we found that these methods share a commonality. In fact, these methods can be uniformly defined as a method for separation of overlapped and non-overlapped light rays. If we need to separate certain components, then we only have to design a non-overlapping projection system for these components.

4.2. Perspective projection

First, we show how the direct and global components change when the illumination and observation settings change in normal perspective projection.

Separation of direct and indirect reflections

The direct components in the original method [10] are the diffuse and specular reflection, while the global components are inter-reflection, subsurface scattering, and volumetric scattering. The red line in Fig. 4 (a) is an example of light path from the projector to the camera. This red line does not overlap with the other paths indicated by the blue line. Because these light paths do not overlap with each other, the high frequency components remain.

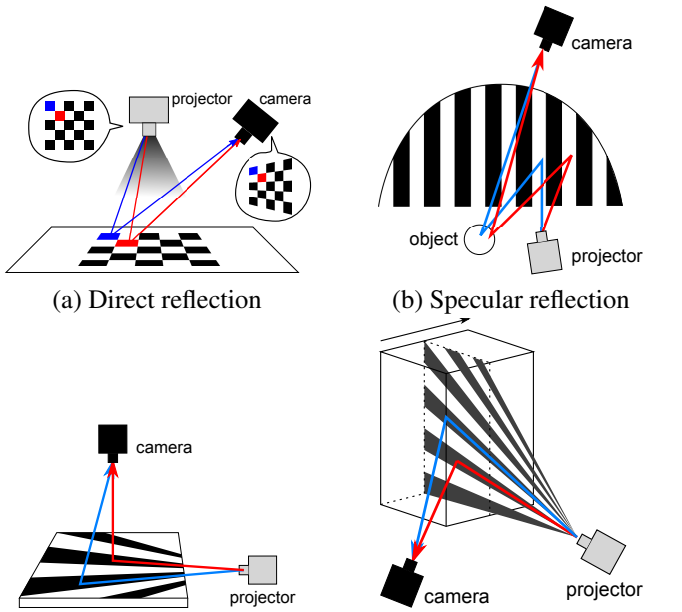

(a) Direct reflection (b) Specular reflection

(c) Planar single scattering (d) Volumetric single scattering

Figure 4. Light extraction by high-frequency illumination.

Separation of diffuse and specular reflections

Lamond *et al*. [6] showed a separation method for diffuse and specular reflections. They projected a stripe pattern on to a hemispherical screen surrounding the object and observed its reflection, as shown in Fig. 4 (b). In this case, the direct component corresponds to the specular reflection and the rays do not overlap with each other.

Separation of single and multiple scatterings in a plane

Mukaigawa *et al*. [8] separated single and multiple scattering components in a thin planar translucent object. They projected a stripe pattern from the side of the object and observed vertically, as shown in Fig. 4 (c). In this case, the direct component corresponds to the single scattering. The important point here is that the target is limited to a plane, and thus each ray is non-overlapped.

Separation of single and multiple scatterings in a volume

Mukaigawa *et al*. [15] extended their previous method for volumetric object. They swept the stripe pattern and observed each depth independently, as shown in Fig. 4 (d).

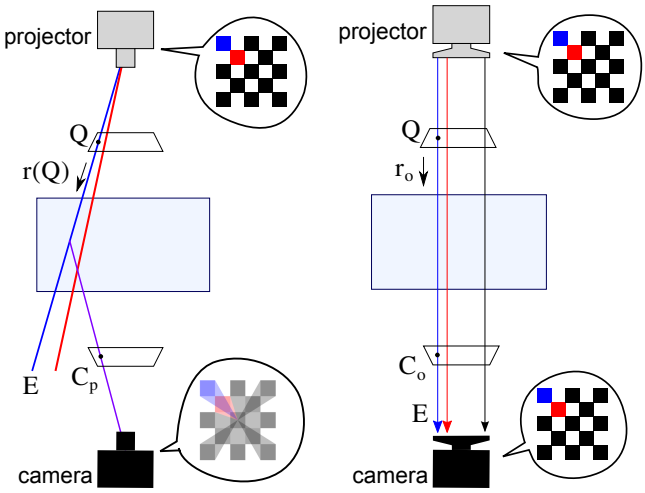

(a) Perspective projection (b) Parallel projection

Figure 5. High frequency illumination to a translucent object.

In this case, the direct component corresponds to the single scattering. If a two-dimensional pattern is projected on a volumetric scene, the single scattering light rays are overlapped in the captured image. This method avoids the overlapping problem by observing each depth independently.

4.3. Parallel projection

Let us assume a simple setting in which a projector and a camera are placed face to face, as shown in Fig. 5 (a). If a normal projector and a normal camera are used for high frequency illumination, the transmissive rays cannot be extracted as a direct component. This is because the transmissive rays are overlapped. Let us consider a light ray $\mathbf{E}$, which corresponds to a pixel $\mathbf{Q}$ in the projection pattern. This ray can be expressed as

$$\mathbf{E} = \mathbf{Q} + t \cdot \mathbf{r}(\mathbf{Q}), \tag{6}$$

where $\mathbf{r}(\mathbf{Q})$ denotes the direction of the ray, which depends on the pixel $\mathbf{Q}$, and t is a parameter. This ray is captured by a camera, and the captured image $\mathbf{C_p}$ is expressed as

$$\mathbf{C_p} = \mathbf{P} \cdot (\mathbf{Q} + t \cdot \mathbf{r}(\mathbf{Q})), \tag{7}$$

where $\mathbf{P}$ denotes the perspective projection matrix of the camera. This shows that a pixel in the projected pattern is observed as a line in the captured image. Therefore, there is no one-to-one correspondence between the projected pattern and the captured image. For example, red and blue lines in the projected pattern produce two rays which do not overlap in the 3-D volume, as shown in Fig. 5 (a). However, the two rays overlap with each other in the image captured by the camera.

On the other hand, parallel projection produces different relationships. Let us assume that the projector and the camera are arranged to produce a coaxial orthographic projection, as shown in Fig. 5 (b). In this case, a ray $\mathbf{E}$ can be expressed as

$$\mathbf{E} = \mathbf{Q} + t \cdot \mathbf{r_o}, \tag{8}$$

where $\mathbf{r_o}$ denotes the direction of the ray, which is the same as the projection direction. It should be noted that $\mathbf{r_o}$ does not depend on the pixel $\mathbf{Q}$. The coordinates in the captured image are expressed as

$$\begin{aligned} \mathbf{C_o} &= \mathbf{O} \cdot (\mathbf{Q} + t \cdot \mathbf{r_o}) \\ &= \mathbf{O} \cdot \mathbf{Q} + t \cdot \mathbf{O}\mathbf{r_o}, \end{aligned}$$

where $\mathbf{O}$ denotes the orthographic projection matrix of the camera. Here, $\mathbf{O}\mathbf{r_o} = 0$ because r_o is degenerated by the projection. Therefore,

$$\mathbf{C_o} = \mathbf{O} \cdot \mathbf{Q}. \tag{9}$$

This shows that the ray is projected as a point in the captured image. For example, the red and blue pixels produce two parallel rays, and they are observed as being different points without overlapping. Therefore, the transmissive and scattered lights can be separated as non overlapped and overlapped rays, respectively. This is the core essence of our Parallel High-frequency Illumination method, which is based on both the angle and position clues.

5. Experiment

5.1. Measuring system

We have constructed a parallel projection system using telecentric lenses, as shown in Fig. 6. We used the digital micromirror device (DMD) projector development kit (Texas Instruments LightCommander) with a telecentric lens (Edmund Optics). This projector has an infra-red (850 nm) light source along with visible RGB light sources.

The CCD camera (Point Grey Grasshopper2) which has sensitivity to the near infra-red light, also has a mounted telecentric lens. Linear polarizers are placed in front of both lenses to reduce scattered lights. Using this equipment, we realized parallel high-frequency illumination in the near infra-red region.

For the high-frequency illumination, a 9px×9px checker pattern is projected. This size provides a threshold to determine the allowed spread of the transmissive lights. The appropriate size depends on the object size, the resolutions of both the camera and the projector, and the optical density. The automatic selection of the most appropriate size is a part of our future work.

(a) Target object (b) Target object is in pure water (c) White pattern of visible light (d) White pattern of near infra-red (e) Proposed method

Figure 7. Experimental results.

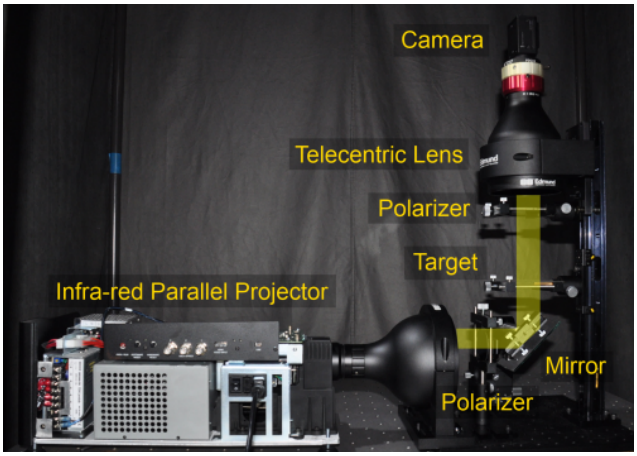

Figure 6. Parallel projection system.

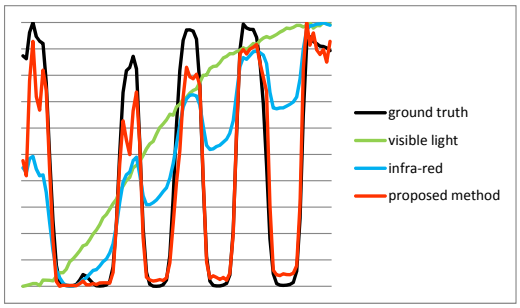

Figure 8. Comparison of intensity profiles.

Table 1. Normalized cross correlation.

Normal illumination in visible light	Normal illumination in near infra-red	Proposed method
-0.10	0.68	0.95

5.2. Experiment with diluted milk

First, we confirmed the descattering effect by the proposed method. The target object is a metallic wire, as shown in Fig. 7 (a). We regard a clear transmissive image which is capured when the target object is in pure water as a ground truth, as shown in Fig. 7(b). Then, a small amount of milk is poured into the water. The density of the diluted milk is 2.2%.

We use two wavelengths of visible (525 nm) and near infra-red (850 nm) light for comparison purposes. Figure 7 (c, d, e) show the experimental results. The image in Fig. 7(c) shows a normal transmissive image in visible light. Because the light is strongly scattered, it is hard to recognize the object. The image in Fig. 7(d) is a normal transmissive image, but in the near infra-red region. The use of near infra-red light contributes to sharpening of the image, but it is insufficient. The image in Fig. 7(e) shows the result of our proposed method. This confirms the image sharpening effect, while it also contains some artifacts due to pattern projection. Figure 8 shows a comparison of the intensity profile of each image along the red line in Fig. 7 (b). We can see that the image from the proposed method has sharp edges and it is similar to the ground truth image. Table 1 shows the result of normalized cross correlation with the ground truth image. The proposed method produces the highest value, which confirms the nobility of it.

Next, we confirm the descattering effect for various milk densities. we use 1.9%, 2.2%, 2.5%, 2.8%, and 3.1% milk density values for our experiment. Figure 9 compares the results of normal illumination with near infra-red light and the proposed method. As the normalized cross correlation with the ground truth is computed for each image. As the density of the solution increases, hence clarity of the transmissive images decreases. All images between 1.9% and 2.8% are clearly sharpened by the proposed method and the correlation value increases. However, at 1.9% density, the normal image is still clear but the result is actually worse, because it contains noise caused by the pattern projection process. On the other hand, for 3.1% density, it is difficult to confirm good result because the level of the transmissive

density	1.9%	2.2%	2.5%	2.8%	3.1%
correlation	0.98	0.68	0.30	0.06	0.01

(a) Normal illumination of near infra-red

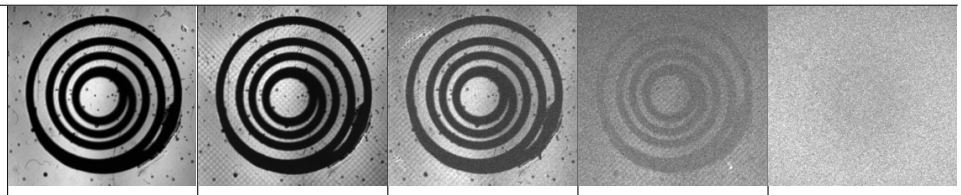

density	1.9%	2.2%	2.5%	2.8%	3.1%
correlation	0.95	0.95	0.84	0.21	0.03

(b) Proposed method

Figure 9. Results for various densities.

light is the same as the level of the camera noise.

5.3. Combination with polarization analysis

Polarizers used in our system are fixed to co-linear. However, our method can be combined with traditional polarization analysis methods. That is, two patterns are captured in co-linear and cross settings, and the difference is used to reduce scattering. Figure 10 is a comparison of our static method and the combined method. The effect of the polarization analysis is much smaller than our proposed method. Although the polarization analysis can be easily combined, the quality is not improved and measuering time becomes two times longer.

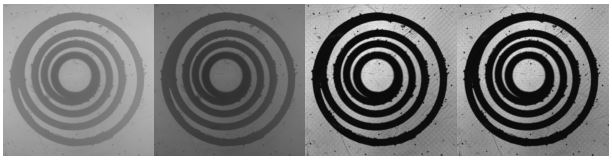

0.916 (a) 0.937 (b) 0.988 (c) 0.988 (d)

Figure 10. Comparison with polarization analysis. Values under the images show cross-correlations with the ground truth.
(a) Normal illumination (b) Traditional polarization analysis (c) Our proposed method (fixed polarizers) (d) Combined method

5.4. Experiments with several scenes

Finally, we apply our method to several scenes, as shown in Fig. 11. We can clearly see the pitch of the screw, the small veins of leaf, and smart card by using the proposed method.

5.5. Discussions and limitations

We confirm that the proposed method is effective for sharpening of transmissive images via several experiments. However, some problems still exist.

First, sometime the image contains large amount of noise. Depending on the particular object, the ratio of transmissive light and scattered light can be quite small. In such a case, the level of the transmissive lights is nearly same as the observation noise level. Therefore, we must have to apply a denoising technique or use a cooled CCD camera. However, this problem is essentially difficult to solve.

Second, the results are degraded if the object surface is not planar. When the surface is round, the light rays refract and break their parallel path. To solve this problem, we must have to devise a method to prevent refraction, e.g. index matching by submerging the target object in a liquid with the same refractive index as the object.

Finally, this method cannot be applied to scenes where there are no transmissive lights. It is therefore impossible to visualize the internal organs of the human body using near infra-red light.

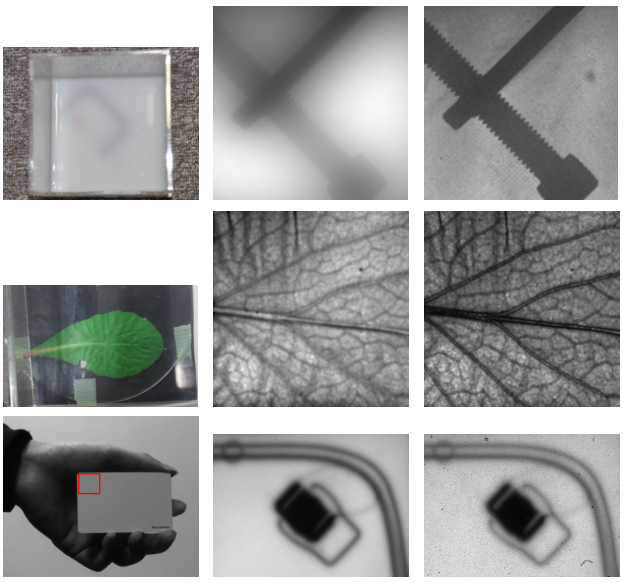

Figure 11. Results for several different scenes.

6. Conclusion

In this paper, we have proposed a new method for the separation of transmissive and scattered lights to sharpen the transmissive image. We have explained the principles of the high-frequency illumination method and the importance of avoiding overlapping rays. We have proposed a new optical design for *Parallel High-frequency Illumination* and have developed a special illumination and observation system using telecentric lenses. The effectiveness of the sharpening process has been confirmed by several experiments and numerical evaluations.

Acknowledgment

This research is granted by the Japan Society for the Promotion of Science (JSPS) through the "Funding Program for Next Generation World-Leading Researchers (NEXT Program)," initiated by the Council for Science and Technology Policy (CSTP).

References

[1] D. Boas and M. A. Franceschini. Near infrared imaging. *Scholarpedia*, 4(4):6997, 2009.

[2] D. Brogioli, A. Vailati, and M. Giglio. A schlieren method for ultra-low-angle light scattering measurements. *Europhysics Letters*, 63(2):220–225, 2003.

[3] C. Fuchs, M. Heinz, M. Levoy, H.-P. Seidel, and H. P. A. Lensch. Combining confocal imaging and descattering. *Computer Graphics Forum, Special Issue for the Eurographics Symposium on Rendering 2008*, 27(4):1245–1253, 6 2008.

[4] G. D. Gilbert and J. C. Pernicka. Improvement of underwater visibility by reduction of backscatter with a circular polarization technique. *Applied Optics*, 6(4):741–746, 1967.

[5] J. Kim, D. Lanman, Y. Mukaigawa, and R. Raskar. Descattering transmission via angular filtering. *Proceeding ECCV'10 Proceedings of the 11th European conference on Computer vision*, pages 86–99, 2010.

[6] B. Lamond, P. Peers, and P. Debevec. Fast image-based separation of diffuse and specular reflections. In *ACM SIGGRAPH 2007 sketches*, SIGGRAPH '07, New York, NY, USA, 2007. ACM.

[7] N. Miura and Y. Sato. Removing skin wrinkles and deblurring veins by using tri-band illumination. *Asian Conference on Computer Vision (ACCV2012)*, 2012.

[8] Y. Mukaigawa, R. Raskar, and Y. Yagi. Analysis of light transport in scattering media. *Computer Vision and Pattern Recognition (CVPR), 2010 IEEE Conference on*, pages 153–160, 2010.

[9] S. G. Narasimhan, S. K. Nayar, B. Sun, and S. J. Koppal. Structured light in scattering media. *Computer Vision, 2005 ICCV 2005 Tenth IEEE International Conference on*, pages 420–427, 2005.

[10] S. K. Nayar, G. Krishnan, M. D. Grossberg, and R. Raskar. Fast separation of direct ang global components of a scene using high frequency illumination. *Proceeding SIGGRAPH '06 ACM SIGGRAPH 2006 Papers*, pages 935–944, 2006.

[11] G. S. Settles. *Schlieren and Shadowgraph Techniques: Visualizing Phenomena in Transparent Media*. Springer, 2001.

[12] T. Treibitz and Y. Y. Schechner. Active polarization descattering. *IEEE Transactions on Pattern Analysis and Machine Intelligence*, 31(3):385–399, 2009.

[13] G. Wetzstein, R. Raskar, and W. Heidrich. Hand-held schlieren photograpy with light field probes. *IEEE Conference on Computational Photography (ICCP)*, 2011.

[14] D. Wu, M. O'Toole, A. Velten, A. Agrawal, and R. Raskar. Decomposing global light transport using time of flight imaging. *Computer Vision and Pattern Recognition (CVPR), 2012 IEEE Conference on*, pages 366–373, 2012.

[15] M. Yasuhiro, R. Ramesh, and Y. Yasushi. Analysis of scattering light transport in translucent media. *IPSJ Transactions on Computer Vision and ApplicationsiCVAj*, 3:122–133, dec 2011.